Eva M. Heppke, Stefan Berendts, Martin Lerch

Crystal structure of mechanochemically synthesized Ag2CdSnS4

Eva M. Heppke, Stefan Berendts and Martin Lerch*

Crystal structure of mechanochemically synthesized Ag$_2$CdSnS$_4$

Abstract: Ag$_2$CdSnS$_4$ was synthesized by a two step mechanochemical synthesis route. From a detailed analysis of the observed reflections in the X-ray powder diffraction pattern, the crystal structure proposed in the literature (space group *Cmc*2$_1$ [E. Parthé, K. Yvon, R. H. Deitch, *Acta Crystallogr.* **1969**, *B25*, 1164–1174; O. V. Parasyuk, I. D. Olekseyuk, L. V. Piskach, S. V. Volkov, V. I. Pekhnyo, *J. Alloys Compd.* **2005**, *399*, 173–177]) is questionable. Our structural investigations presented in this contribution point to the fact that Ag$_2$CdSnS$_4$ crystallizes in the monoclinic wurtzkesterite-type structure (space group *Pn*). At around *T* = 200°C, a phase transition to the orthorhombic wurtzstannite-type structure (space group *Pmn*2$_1$) is observed.

1 Introduction

$A_2^{I}B^{II}C^{IV}X_4$ (X^{2-} = S, Se, Te) compounds are semiconductors exhibiting either a cubic or a hexagonal diamond-related structure [1–3]. The most prominent group of $A_2^{I}B^{II}C^{IV}X_4$ semiconductors are Cu-bearing compounds [4–9]. Among them, Cu$_2$ZnSnS$_4$ has gained much attention as a potential candidate for absorber layers in thin film solar cells [10–12]. Ag-containing compounds are more difficult to synthesize and less stable. Nevertheless, a few $A_2^{I}B^{II}C^{IV}X_4$ phases with A = Ag are known so

*Corresponding author: Martin Lerch,** Institut für Chemie, Technische Universität Berlin, Straße des 17. Juni 135, 10623 Berlin, Germany, Fax: +493031479656, E-mail: martin.lerch@tu-berlin.de
Eva M. Heppke and Stefan Berendts: Institut für Chemie, Technische Universität Berlin, Straße des 17. Juni 135, 10623 Berlin, Germany

far [4, 13–19]. For most Ag compounds, a stannite- or wurtzstannite-/wurtzkesterite-type structure has been presented in the literature. However, there are some compounds that deviate from these two structures. For Ag$_2$CdSnS$_4$, the space group *Cmc*2$_1$ is proposed which can be considered as a hexagonal diamond-/wurtzite-derived structure with a statistical distribution of Ag, Cd, and Sn on Wyckoff position 4*a* with (0, 0.167, 0.370); sulfur is located at another 4*a* position with (0, 0.176, 0.997) [4, 20]. The results of our investigations on the aforementioned compound indicate a different crystal structure. Due to additional reflections in the X-ray powder diffraction pattern of our synthesized sample, space group *Cmc*2$_1$ can be excluded. Ag$_2$CdSnS$_4$ was synthesized via a mechanochemical process which has proven its suitability for the successful preparation of phase-pure and well crystallized quaternary $A_2^{I}B^{II}C^{IV}S_4$ compounds such as Cu$_2$ZnSnS$_4$ [21]. The crystal structure of our mechanochemically prepared Ag$_2$CdSnS$_4$ has been determined using powder X-ray diffraction. Additionally, UV/Vis and DTA measurements were performed. Surprisingly, a phase transition at around *T* = 200°C could be observed and the crystal structures of both the high- and low-temperature phases were investigated by *in-situ* XRD.

2 Results and discussion

The mechanochemical synthesis approach with a subsequent annealing step as described in the experimental section results in the formation of phase-pure and well crystallized Ag$_2$CdSnS$_4$. Phase composition was determined by EDX and combustion analysis and is in accordance with the theoretical one (Table 1). EDX mapping also confirmed a homogenous distribution of Ag, Cd, Sn, and S in the individual particles (Fig. 1).

Interestingly, in the DTA curve of our Ag$_2$CdSnS$_4$ sample thermal effects were observed. An endothermic peak occurs in the heating process (T_p = ~205°C) and an exothermic one is observed during cooling (T_p = ~199°C). This points to a reversible phase transition at around 200°C (Fig. 2). The reversibility of the phase transition was also proven by *in-situ* X-ray diffraction.

Table 1: Phase composition of Ag_2CdSnS_4 calculated from EDX data and sulfur content determined by elemental analysis.

Ag_2CdSnS_4		
	Ideal (wt.-%)	Measured (wt.-%)
Ag	37.5	36.4
Cd	19.5	20.7
Sn	20.6	21.2
S (EDX)	22.3	21.7
S (EA)	22.3	22.0

2.1 Structural relationship between hexagonal diamond and the wurtzstannite-/wurtzkesterite-type structure

As it can be seen in the Bärnighausen tree [22, 23], elucidating the relationship between the hexagonal diamond (lonsdaleite) and the wurtzstannite-/wurtzkesterite-type structures (Fig. 3), space group $Cmc2_1$, as a subgroup to that of the wurtzite-type structure, is proposed either for binary compounds as well as for compounds with a statistical distribution of their cations/anions on one position. For Ag_2CdSnS_4, space group $Cmc2_1$ is mentioned in the literature with Ag, Cd, and Sn distributed statistically on the position $4a$ with (0, 0.167, 0.370) and S on another $4a$ position with (0, 0.176, 0.997) [20].

Similar compounds containing silver either crystallize in cubic diamond/sphalerite-related structures such as the stannite- or kesterite-type structure (such as Ag_2ZnSnS_4 [14], Ag_2FeSnS_4 [13], Ag_2ZnGeS_4 [24]) or in crystal structures derived from the hexagonal diamond/wurtzite type providing non-equivalent positions for the cations/anions

(the wurtzstannite-type structure (space group $Pmn2_1$) and its derivatives with space group Pn (wurtzkesterite-type structure) or $Pna2_1$). Compounds crystallizing in the wurtzstannite-type structure are Ag_2CdGeS_4 [4] and Ag_2HgSnS_4 [15], whereas Ag_2MnSnS_4 [18] and Si-bearing compounds such as Ag_2FeSiS_4 [16] and Ag_2ZnSiS_4 [17] crystallize in the wurtzkesterite-type structure. Due to the close structural relationships between these three structures, it can be quite difficult to distinguish between them when using conventional methods. For Ag_2CdGeS_4, two polymorphs have been reported exhibiting the space groups $Pmn2_1$ [4] and $Pna2_1$ [25], respectively.

2.2 The high-temperature phase of Ag_2CdSnS_4

Starting with the high-temperature phase, it should be noted that an orthorhombic unit cell could be found by the Werner algorithm using the program WINXPOW 1.2 (STOE & Cie GmbH, Darmstadt, Germany) [29] for the sample at $T = 300°C$. The lattice parameters were refined to $a = 8.2263$ Å, $b = 7.0655$ Å, and $c = 6.7051$ Å leaving no reflection behind. The volume of the unit cell was calculated to 389.7 Å³. It should be mentioned that the lattice parameter a given by the Werner algorithm is two times larger than that of the proposed crystal structure with space group $Cmc2_1$ for Ag_2CdSnS_4 [4, 20]. Examples of $A_2^IB^{II}C^{IV}X_4$ compounds with a lattice parameter a of around 8.23 Å (and similar values for the lattice parameters b and c) within the orthorhombic crystal system have also been described by other authors [15].

For the Rietveld refinement of the high-temperature phase space group $Pmn2_1$ (wurtzstannite-type structure)
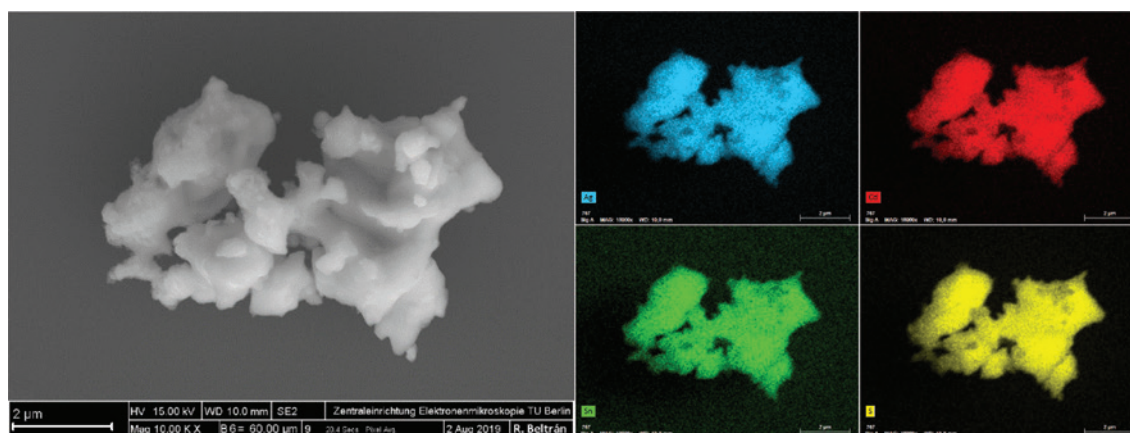
Fig. 1: SEM images of Ag_2CdSnS_4 particles and EDX mapping of homogenously distributed Ag (blue), Cd (red), Sn (green), and S (yellow) in the Ag_2CdSnS_4 particles.

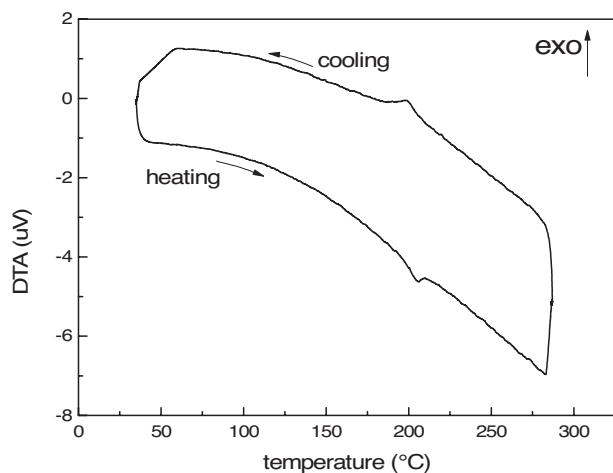**Fig. 2:** DTA curve of Ag_2CdSnS_4 under nitrogen atmosphere.

is used. As depicted in Fig. 4, the experimental pattern is in good agreement with the theoretical one. Crystallographic details as well as atomic and structural parameters are listed in Tables 2 and 3. The Debye Waller factors of sulfur were set to a value of 1 and not refined, also the site occupation factors of all atoms. As $Pmn2_1$ is a polar space group and therefore possesses one origin-free direction (the z direction), the z parameter of the Ag atom position was fixed. As Ag, Cd, and Sn are not distinguishable using conventional X-ray diffraction methods, the distribution of these cations in the wurtzstannite- (and also wurtzkesterite-) type structure was set to that of the related compounds described in the literature.

The wurtzstannite-type structure (space group $Pmn2_1$) of the high-temperature phase of Ag_2CdSnS_4 can be described as a hexagonal diamond/wurtzite-derived structure with a hexagonal closest packing of sulfur anions. Ag is located at a fourfold position whereas Cd and Sn occupy two non-equivalent twofold positions. Three crystallographically independent sulfur positions are present, where S1 is located on a fourfold position and S2 as well as S3 atoms occupy two twofold positions. Considering the honeycomb set-up, the wurtzstannite-type structure is built up of consecutive Ag and Cd/Sn layers (in general: A^I and B^{II}/C^{IV} layers). This is manifested in alternating layers of Ag-centered and Cd/Sn-centered polyhedra along the b axis (Fig. 5). These alternating stacking sequence appears to be in line with that of the stannite type [5, 30], the analogous structure type derived from the cubic diamond/sphalerite-type structure. All atoms in the wurtzstannite-type structure are surrounded tetrahedrally. Each cation is coordinated by two S1 atoms, one S2 atom, and one S3 atom. The sulfur atoms are coordinated by two Ag and one Cd atom as well as one Sn atom.

2.3 The low-temperature phase of Ag_2CdSnS_4

For the crystal structure determination of the low-temperature phase, all four direct subgroups of $Pmn2_1$ ($P2_1$, Pm, Pn, and $Pna2_1$) (Fig. 6) were considered and tested as refinement models. For example, the symmetry reduction from space group $Pmn2_1$ to Pn is expressed by the splitting of the fourfold Ag atom position $4b$ into two non-equivalent twofold positions $2a$. The atomic and lattice parameters for the refinements in the four subgroups were generated by the program TRANSTRU found on the Bilbao Crystallographic Server [31–33]. For the space groups $Pna2_1$ and Pn, we also used reported structural parameter of related compounds [25, 28] as starting values in the Rietveld refinements.

In the subgroups $P2_1$, Pm, and $Pna2_1$ convergence problems occurred during the refinements (profile, atomic positions, Debye-Waller factors). However, a successful refinement was achieved in space group Pn, the wurtzkesterite-type structure. The experimental diffraction pattern is in good agreement with the theoretical one (Fig. 7). Crystallographic details are summarized in Table 2; atomic and structural parameters are presented in Table 4. The Debye-Waller factors of the sulfur atoms were kept fixed at a value of 1, and the site occupation factors were not refined. Space group Pn also belongs to the group of polar/origin-free space groups. This particular space group exhibits two origin-free directions (x and z). For the refinement in Pn, the x and z parameters of the Ag1 atom position were kept fixed to define the origin.

The low-temperature phase of Ag_2CdSnS_4 crystallizes in the space group Pn (wurtzkesterite-type structure) with $a = 6.704$, $b = 7.038$, $c = 8.217$ Å, and $\beta = 90.16°$. The wurtzkesterite-type structure can be derived from the hexagonal diamond structure and is composed of a hexagonal closest packed arrangement of the sulfur anions (Fig. 8). The crystal structure contains two independent Ag positions Ag1 and Ag2, one Cd, and one Sn position where all cations are located on twofold positions. This setup occurs also for the anions with in total four independent sulfur positions on twofold positions. Keeping in mind the honeycomb set-up, alternating Ag/Cd and Ag/Sn layers (in general A^I/B^{II} and A^I/C^{IV} layers) are distinguishable which is analogous to the kesterite-type structure [5] derived from the cubic diamond structure. Interatomic Ag–S distances range from 2.46(3) to 2.52(4) Å with an average of 2.50 Å for Ag1–S and from 2.52(3) to 2.58(2) Å with an average of 2.55 Å for Ag2–S. The Ag–S bond lengths correlate quite well with those known from Ag_2CdGeS_4 (Ag–S: 2.52–2.57 Å) [34] and are slightly smaller than those reported for Ag_2FeSiS_4
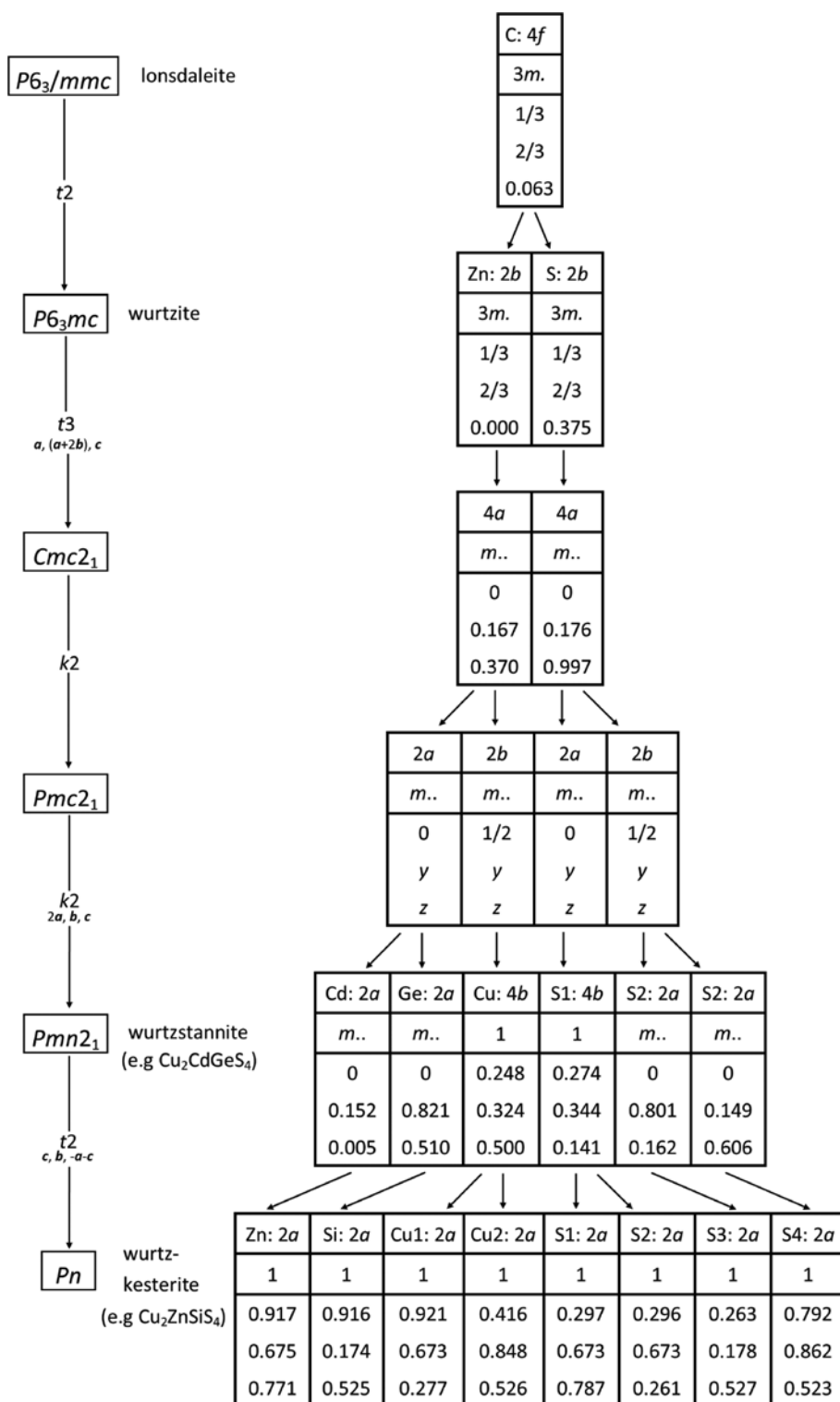
Fig. 3: Group-subgroup scheme (Bärnighausen formalism) for the group-theoretical relation between hexagonal diamond (lonsdaleite) and the wurtzstannite-/wurtzkesterite-type structure with data taken from [26] for lonsdaleite, [27] for wurtzite, [20] for space group $Cmc2_1$, [4] for wurtzstannite-type Cu_2CdGeS_4, and [28] for wurtzkesterite-type Cu_2ZnSiS_4.

(Ag1–S: 2.52–2.58 Å; Ag2–S: 2.54–2.61 Å) [16]. Cd–S bond lengths range from 2.51(3) to 2.58(3) Å with an average of 2.55 Å and are in good agreement with those found in Cu_2CdGeS_4 (Cd–S: 2.51–2.60 Å) [4] and Ag_2CdGeS_4 (Cd–S: 2.49–2.57 Å) [34]. Interatomic Sn–S distances vary from 2.39(3) to 2.51(3) Å and are in average 2.43 Å which is

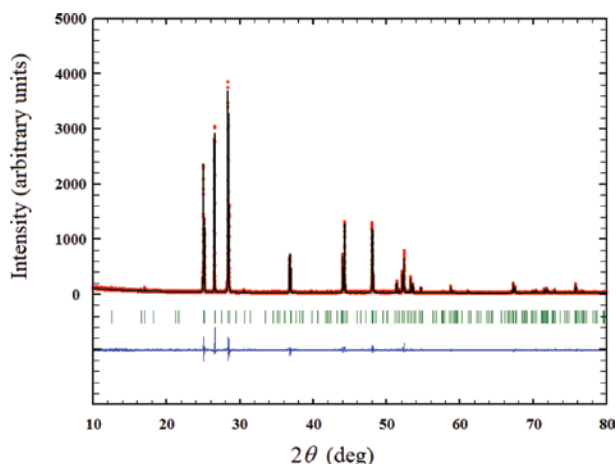**Fig. 4:** X-ray diffraction pattern of the high-temperature phase (measured at $T = 300°C$) of Ag$_2$CdSnS$_4$ with the results of the Rietveld refinement in space group $Pmn2_1$ (red: measured; black: calculated; blue: measured−calculated).

somewhat longer than those in Li$_2$CdSnS$_4$ (Sn−S: 2.38–2.39 Å) [35] and Li$_2$ZnSnS$_4$ (Sn−S: 2.35–2.42 Å) [36].

2.4 Stabilization of the high-temperature phase at room temperature

The observed phase transition seems to be of first order. Consequently, it is no surprise that the stabilization of the high-temperature phase of Ag$_2$CdSnS$_4$ at room temperature

was feasible by annealing the sample at $T = 300°C$ for 3 h in an evacuated and closed silica tube in a vertically positioned tube furnace (Nabertherm RT 50-250/13; C450 controller) and subsequently quenching it in dry ice. Rietveld refinements were done in space group $Pmn2_1$ as well as in Pn and confirmed that the quenched sample crystallizes in the orthorhombic space group $Pmn2_1$. As expected, the difference of the residual values R_{wp} between the space groups $Pmn2_1$ and Pn is not significant ($R_{wp} = 10.9$ for $Pmn2_1$ and $R_{wp} = 10.7$ for Pn, respectively). Additionally, convergence problems occurred for the refinement in space group Pn. The powder diffraction pattern of the stabilized high-temperature phase of Ag$_2$CdSnS$_4$ quenched to room temperature is shown in Fig. 9. Crystallographic details as well as atomic and structural parameters are presented in Tables 2 and 5. The refinement strategy was similar to that of the sample measured *in-situ*.

The interatomic Ag–S distances in the quenched high-temperature phase vary from 2.505(12) to 2.521(15) Å with an average of 2.52 Å and correlate well with the Ag1–S distances (2.46(3)–2.52(4) Å) found in the low-temperature phase of Ag$_2$CdSnS$_4$. However, they are somewhat smaller than the Ag2–S distances (2.52(3)–2.58(2) Å) reported for Ag$_2$CdGeS$_4$ (Ag–S: 2.52–2.57 Å) [34] and Ag$_2$FeSiS$_4$ (Ag1–S: 2.52–2.58 Å; Ag2–S: 2.54–2.61 Å) [16]. Cd–S bond lengths range from 2.531(17) to 2.59(3) Å with an average value of 2.56 Å. This correlates pretty well with reported Cd–S distances for Cu$_2$CdGeS$_4$ (Cd–S: 2.51–2.60 Å) [4] and Ag$_2$CdGeS$_4$ (Cd–S: 2.49–2.57 Å) [34] as well with the ones in our

Table 2: Results of the refinements for the high- and low-temperature phases of Ag$_2$CdSnS$_4$ (standard deviations in parenthesis).

	Ag$_2$CdSnS$_4$		
	High-temperature phase $T = 300°C$	Quenched high-temperature phase at r. t.	Low-temperature phase
Crystal system	Orthorhombic	Orthorhombic	Monoclinic
Space group	$Pmn2_1$	$Pmn2_1$	Pn
Z	2	2	2
Unit cell dimensions	$a = 8.2171(6)$ Å	$a = 8.2137(4)$ Å	$a = 6.7036(2)$ Å
	$b = 7.0641(5)$ Å	$b = 7.0403(4)$ Å	$b = 7.0375(3)$ Å
	$c = 6.7029(5)$ Å	$c = 6.7033(2)$ Å	$c = 8.2166(3)$ Å
			$\beta = 90.1577(9)°$
Cell volume, Å³	389.08(5)	387.63(3)	387.63(2)
Calculated density, g cm^{-3}	4.91	4.93	4.93
Diffractometer	RIGAKU SmartLab 3 kW system		
Radiation	Cu$K\alpha_1$ radiation		
Wavelength, Å	$\lambda = 1.54060$ Å		
Number of refined parameters	34	34	48
R_p	0.096	0.081	0.100
R_{wp}	0.128	0.109	0.138
R_{exp}	0.138	0.098	0.152
R_{Bragg}	0.049	0.049	0.050
S	0.93	1.13	0.91

Table 3: Refined atomic parameters for the high-temperature phase ($T = 300°C$) of Ag$_2$CdSnS$_4$ in space group $Pmn2_1$ (standard deviations in parenthesis).
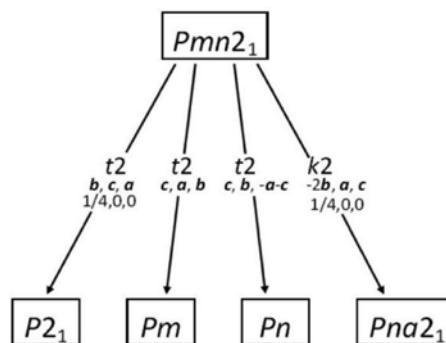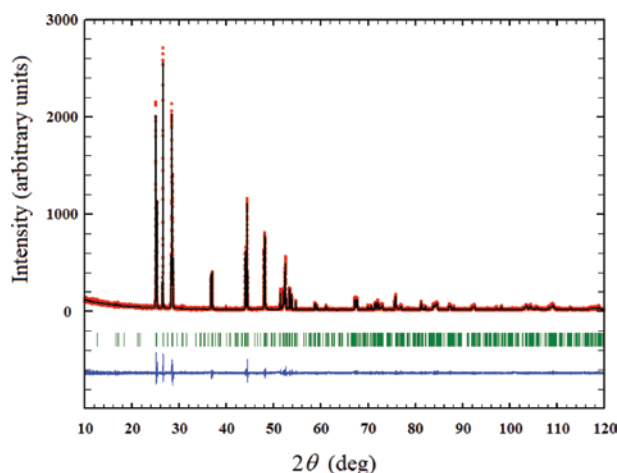
Atom	Wyckoff	x	y	z	s.o.f	B_{iso} (Å²)
Ag	4b	0.2543(7)	0.3242(7)	−0.01018[a]	1	3.8(2)
Cd	2a	0	0.8440(10)	0.988(3)	0.5	5.3(3)
Sn	2a	0	0.1770(8)	0.487(3)	0.5	1.0(2)
S1	4b	0.239(2)	0.336(2)	0.378(3)	1	1
S2	2a	0	0.180(4)	0.834(3)	0.5	1
S3	2a	0	0.855(4)	0.363(4)	0.5	1

[a]Fixed z value.

Fig. 6: Group-theoretical relation (Bärnighausen formalism) between space group $Pmn2_1$ (wurtzstannite-type structure) and its direct subgroups $P2_1$, Pm, Pn, and $Pna2_1$.

Fig. 7: X-ray diffraction pattern of the low-temperature phase (measured at $T = 25°C$) of Ag$_2$CdSnS$_4$ with the results of the Rietveld refinement in space group Pn (red: measured; black: calculated; blue: measured−calculated).

low-temperature phase of Ag$_2$CdSnS$_4$ (2.51(3)–2.58(3) Å). For the Sn–S distances, the values vary from 2.39(3) to 2.491(17) Å with an average of 2.45 Å. They are in agreement with those found in the low-temperature phase (2.39(3)–2.51(3) Å) and also with those reported for Li$_2$CdSnS$_4$ (Sn–S: 2.38–2.39 Å) [35] and Li$_2$ZnSnS$_4$ (Sn–S: 2.35–2.42 Å) [36].

For the high- and the low-temperature phase of our Ag$_2$CdSnS$_4$ sample, additional refinements were undertaken in different space groups. These include the centrosymmetric space group $Pnma$ as well as the non-centrosymmetric space group $Pmc2_1$. In addition, refinements in the triclinic crystal system have been performed. All refinements in these aforementioned space groups resulted in severe convergence problems. Consequently, we exclude all these space groups as possible candidates for Ag$_2$CdSnS$_4$.

Rietveld refinements in $Pmn2_1$ and Pn were done for all temperatures (25–300°C, 25 K steps). The monoclinic angle β was plotted against the temperature for the whole temperature range (black dots in Fig. 10). The plotted results point to the fact that β abruptly becomes 90°, the value of the orthorhombic high-temperature phase, at about 200°C. This again indicates a first order
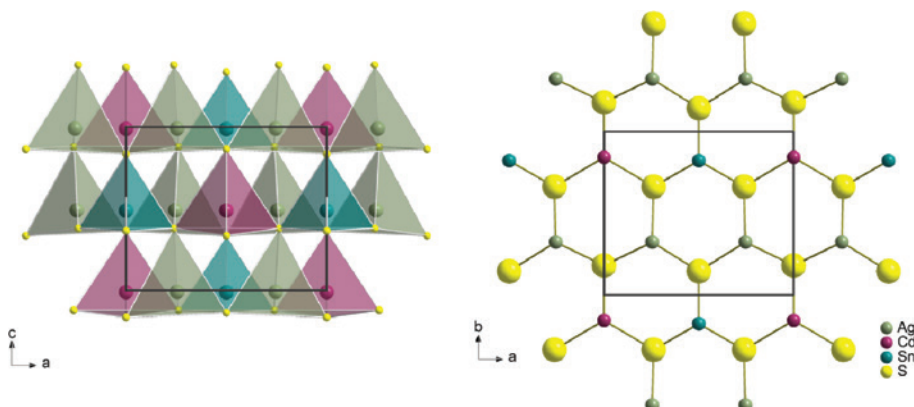

Fig. 5: Crystal structure of the high-temperature phase of Ag$_2$CdSnS$_4$ ($Pmn2_1$) with cation-centered polyhedra viewed along the [010] direction (left) and the honeycomb set-up with stacking sequence of alternating Ag and Cd/Sn layers viewed along the [001] direction (right).

Table 4: Refined atomic parameters for the low-temperature phase of Ag$_2$CdSnS$_4$ ($T = 25°$C) in space group Pn (standard deviations in parenthesis).

Atom	Wyckoff	x	y	z	s.o.f	B_{iso} (Å^2)
Ag1	2a	0.91670[a]	0.675(4)	0.27782[a]	1	1.5(6)
Ag2	2a	0.407(3)	0.8454(8)	0.533(3)	1	2.5(3)
Cd1	2a	0.913(2)	0.674(4)	0.773(3)	1	1.99(6)
Sn1	2a	0.908(2)	0.1759(7)	0.523(2)	1	0.22(13)
S1	2a	0.298(7)	0.665(7)	0.783(4)	1	1
S2	2a	0.284(6)	0.669(8)	0.278(5)	1	1
S3	2a	0.267(4)	0.182(3)	0.526(5)	1	1
S4	2a	0.791(4)	0.851(3)	0.521(4)	1	1

[a]Fixed x and z values.

transition from the wurtzkesterite-type structure to the wurtzstannite-type structure. The area around 200–225°C may be considered as two-phase region. The error bars at temperatures ≤200°C are smaller than those >200°C. For the refined cell volume, no significant jump in the region around 200°C can be observed (red squares in Fig. 10).

2.5 UV/Vis spectroscopy

The optical properties of Ag$_2$CdSnS$_4$ were measured in reflectance mode, and the optical band gaps were determined using the Tauc plot method [37, 38]. For the direct optical band gap a value of $E_g = 1.93$ eV was calculated whereas a narrower indirect optical band gap of $E_g = 1.82$ eV was obtained (Fig. 11). The color of our sample (black with violet accents) points to a direct optical band gap of $E_g = 1.93$ eV which is in good agreement with the experimentally determined band gap mentioned in literature [39].
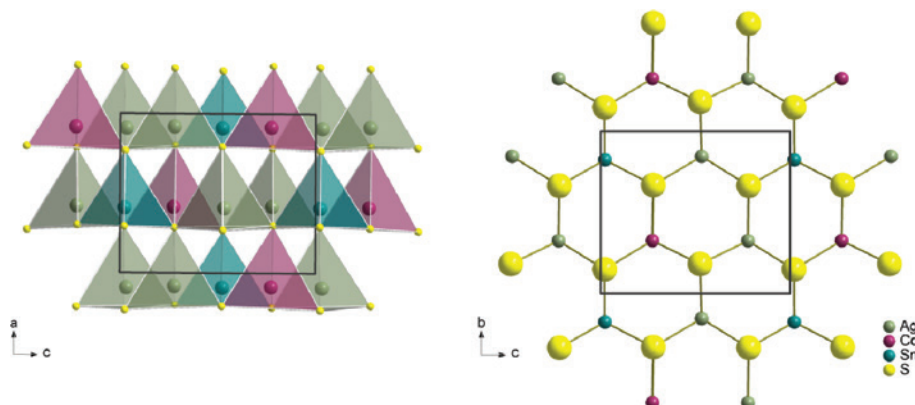

Fig. 9: X-ray diffraction pattern of the high-temperature phase of Ag$_2$CdSnS$_4$ stabilized at room temperature with the results of the Rietveld refinement in space group $Pmn2_1$ (red: measured; black: calculated; blue: measured–calculated).

3 Conclusions

Phase-pure and well crystallized Ag$_2$CdSnS$_4$ was synthesized by ball milling (350 rpm, 5 h) and subsequent annealing at $T = 550°$C under H$_2$S atmosphere for 2 h in a tube furnace. The observed reflections in the X-ray powder diffraction pattern are not in agreement with the crystal structure proposed in literature (space group $Cmc2_1$) where all cations are statistically distributed on one position. Structural investigations including Rietveld refinements using our mechanochemically prepared Ag$_2$CdSnS$_4$ sample point, in accordance to the calculations of Chen et al. [42], to the presence of the wurtzkesterite-type structure (space group Pn) with an ordered arrangement of the cations. A reversible

Fig. 8: Crystal structure of the low-temperature phase of Ag$_2$CdSnS$_4$ crystallizing in space group Pn with cation-centered polyhedra (view along the [0$\bar{1}$0] direction, left) and the honeycomb set-up with a stacking sequence of alternating Ag/Cd and Ag/Sn layers viewed along the [100] direction.
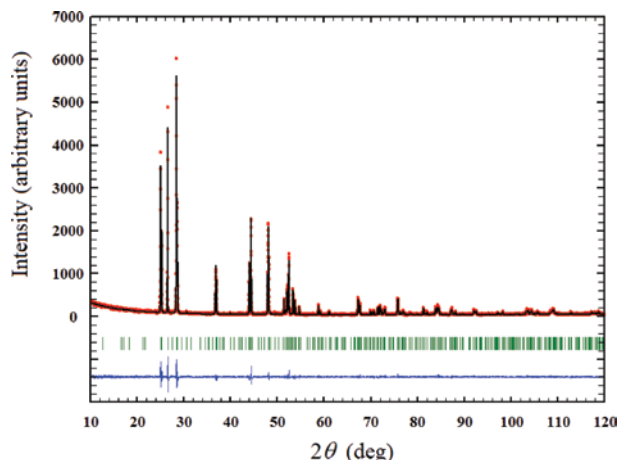
Table 5: Refined atomic parameters for the high-temperature phase of Ag_2CdSnS_4 in space group $Pmn2_1$ quenched to room temperature (standard deviations in parenthesis).

Atom	Wyckoff	x	y	z	s.o.f	B_{iso} (Å²)
Ag1	4b	0.2532(9)	0.3255(8)	−0.00662[a]	1	1.5(2)
Cd1	2a	0	0.8445(11)	0.983(3)	0.5	2.4(3)
Sn1	2a	0	0.1767(9)	0.491(3)	0.5	0.28(15)
S1	4b	0.251(3)	0.337(3)	0.368(5)	1	1
S2	2a	0	0.184(4)	0.847(4)	0.5	1
S3	2a	0	0.851(4)	0.369(6)	0.5	1

[a]Fixed z value.
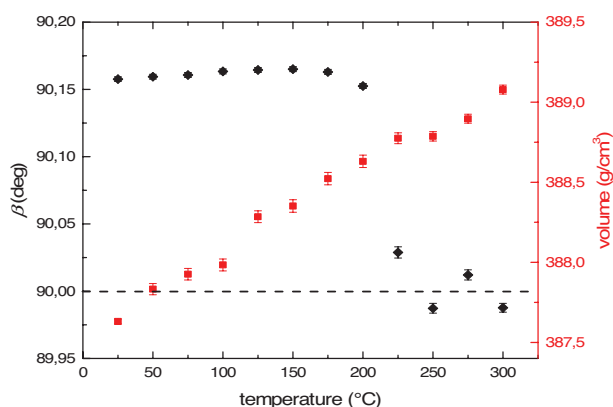
Fig. 10: Monoclinic angle β and cell volume plotted against temperature (from Rietveld refinements in space group Pn for β and from refinements in Pn ($T \leq 200°C$) and $Pmn2_1$ ($T > 200°C$) for the cell volume).

first-order phase transition at around 200°C from a low-temperature wurtzkesterite- to a high-temperature wurtzstannite-type structure has been observed. Additionally, a direct optical band gap of $E_g = 1.93$ eV, which is in agreement to that reported in the literature, was found. In the present work, the mechanochemical synthetic route was again successful for the preparation of

phase-pure multinary sulfides. This particular way of synthesis appears to have a strong effect on the crystal structure of the resulting compounds. This may be an explanation for our different observations compared to the literature results presented in [4, 20].

4 Experimental Section

4.1 Synthesis

Ag_2CdSnS_4 was synthesized by ball milling in a high-energy planetary Mono Mill (Pulverisette 6, Fritsch, Idar-Oberstein, Germany), followed by an annealing step under an atmosphere of H_2S. As starting materials Ag_2S (Schuchardt), CdS, SnS, and sulfur (Fluka, 99.99%) were used which were filled in a 45 mL zirconia-made grinding beaker with 6 zirconia balls with a diameter of 15 mm. A rotational speed of 350 rpm and a milling time of 5 h were set. In order to obtain a highly crystalline product, the grounded powder was annealed at $T = 550°C$ for 2 h under H_2S atmosphere. A 0.1 м $Cd(CH_3CO_2)_2$ solution and H_2S (Air Liquide, 99.5%) were used for precipitation of CdS. SnS was synthesized using the high-temperature solid-state reaction of the elements tin (Merck, 99.9%) and sulfur (Fluka, 99.99%) in an evacuated and sealed SiO_2 ampoule.

4.2 Structural and chemical characterization

X-ray powder diffraction investigations as well as *in-situ* high-temperature X-ray diffraction experiments (25–300°C, N_2 atmosphere) were carried out with a RIGAKU SmartLab 3 kW system equipped with a Kα1 unit (Johansson-type Ge crystal, Cu$K\alpha_1$ radiation, $\lambda = 1.54060$ Å). The diffraction data were obtained in Bragg-Brentano geometry over an angular range
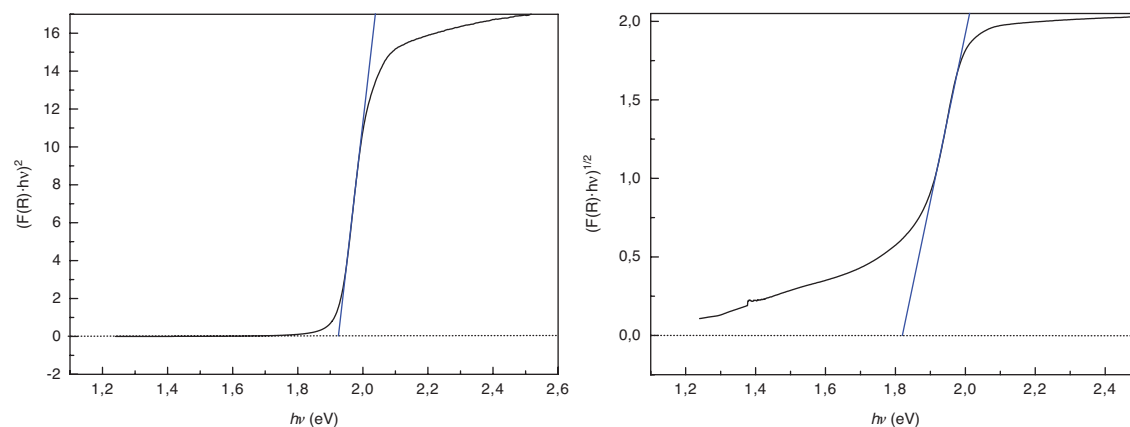
Fig. 11: UV/Vis spectra of Ag_2CdSnS_4 with Tauc plot determinations of the direct (left) and indirect (right) optical band gap.

of $2\theta = 10–120°$ for room temperature and $2\theta = 10–80°$ for high-temperature measurements. Rietveld refinements [40] were performed using the program FULLPROF [41] by applying a pseudo-Voigt function. Backgrounds were fitted using a set of various background points with refinable heights. It should be mentioned that anisotropic strain broadening terms were used due to anisotropic reflection broadening.

Further details of the crystal structure investigation may be obtained from Fachinformationszentrum Karlsruhe, 76344 Eggenstein-Leopoldshafen, Germany (fax: +49-7247-808-666; e-mail: crysdata@fiz-karlsruhe.de, http://www.fiz-informationsdienste.de/en/DB/icsd/depot_anforderung.html) on quoting the deposition numbers CSD-1979198 and CSD-1979199.

For the chemical characterization of Ag_2CdSnS_4, energy dispersive X-ray spectroscopy (EDX) using a DSM 982 GEMINI spectrometer (Carl Zeiss AG, Oberkochen, Germany) equipped with a XFlash 6|60 detector (Bruker, Billerica, USA) were performed. For the determination of the sulfur content, an instrumental error of 5% is given. The EDX measurements were carried out at the Zentrum für Elektronenmikroskopie (ZELMI) of the TU Berlin. For the confirmation of the sulfur content, additional analyses were carried out using a FlashEA 1112 elemental analyzer (Thermo Scientific™, Waltham, USA). Hereby, a device error of 2% is assumed.

Thermoanalytical analysis (DTA) were carried out using a STA 7300 thermogravimeter (Hitachi, Chiyoda, Japan). These measurements were performed under nitrogen atmosphere up to 300°C with a heating and cooling rate of 3 K min^{-1}; alumina crucibles were used as reference and sample container.

4.3 UV/Vis spectroscopy

The optical band gaps were determined by UV/Vis measurements using a V670 UV/Vis-NIR spectrometer (Jasco Deutschland GmbH, Pfungstadt, Germany). The spectra obtained in diffuse reflectance mode were converted into absorption spectra by the Kubelka-Munk function; the optical band gaps were received from the absorption spectra using the Tauc plot method [37, 38]. The standard deviation for E_g was estimated close to 0.05 eV. For sample preparation, Ag_2CdSnS_4 was mixed with a white standard (MgO) in a mass ratio of 1:1.

References

[1] C. H. L. Goodman, *J. Phys. Chem. Solids* **1958**, *6*, 305–314.

[2] B. R. Pamplin, *Nature* **1960**, *188*, 136–137.

[3] B. R. Pamplin, *J. Phys. Chem. Solids* **1964**, *25*, 675–684.

[4] E. Parthé, K. Yvon, R. H. Deitch, *Acta Crystallogr.* **1969**, *B25*, 1164–1174.

[5] S. R. Hall, J. T. Szymanski, J. M. Stewart, *Can. Mineral.* **1978**, *16*, 131–137.

[6] W. Schäfer, R. Nitsche, *Mater. Res. Bull.* **1974**, *9*, 645–654.

[7] A. F. Moodie, H. J. Whitfield, *Acta Crystallogr.* **1986**, *B42*, 236–247.

[8] B. Lui, M. Zhang, Z. Zhao, H. Zeng, F. Zheng, G. Guo, J. Huang, *J. Solid State Chem.* **2013**, *204*, 251–256.

[9] I. D. Olekseyuk, O. V. Marchuk, L. D. Gulay, O. Y. Zhbankov, *J. Alloys Compd.* **2005**, *398*, 80–84.

[10] K. Ito, T. Nakazawa, *Jpn. J. Appl. Phys.* **1988**, *27*, 2094–2097.

[11] H. Katagiri, K. Saitoh, T. Washio, H. Shinohara, T. Kurumadani, S. Miyajima, *Sol. Energy Mater. Sol. Cells* **2001**, *65*, 141–148.

[12] J. Seol, S. Lee, J. Lee, H. Nam, K. Kim, *Sol. Energy Mater. Sol. Cells* **2003**, *75*, 155–162.

[13] R. Caye, Y. Laurent, P. Picot, R. Pierrot, C. Lévy, *Bull. Minéral.* **1968**, *91*, 383–387.

[14] Z. Johan, P. Picot, *Bull. Minéral.* **1982**, *105*, 229–235.

[15] H. Haeuseler, M. Himmrich, *Z. Naturforsch.* **1989**, *44b*, 1035–1036.

[16] C. D. Brunetta, J. A. Brant, K. A. Rosmus, K. M. Henline, E. Karey, J. H. MacNeil, J. A. Aitken, *J. Alloys Compd.* **2013**, *574*, 495–503.

[17] C. D. Brunetta, B. Karuppannan, K. A. Rosmus, J. A. Aitken, *J. Alloys Compd.* **2012**, *516*, 65–72.

[18] S. Greil, Untersuchungen an ternären und quaternären Kupfer-, Lithium- und Silbersulfiden mit Diamantstruktur. *Dissertation*, Universität Regensburg, Regensburg **2015**.

[19] C. L. Teske, *Z. Naturforsch.* **1979**, *34b*, 544–547.

[20] O. V. Parasyuk, I. D. Olekseyuk, L. V. Piskach, S. V. Volkov, V. I. Pekhnyo, *J. Alloys Compd.* **2005**, *399*, 173–177.

[21] A. Ritscher, J. Just, O. Dolotko, S. Schorr, M. Lerch, *J. Alloys Compd.* **2016**, *670*, 289–296.

[22] H. Bärnighausen, *MATCH Commun. Math. Chem.* **1980**, *9*, 139–175.

[23] U. Müller, *Z. Anorg. Allg. Chem.* **2004**, *630*, 1519–1537.

[24] O. V. Parasyuk, A. O. Fedorchuk, Y. M. Kogut, L. V. Piskach, I. D. Olekseyuk, *J. Alloys Compd.* **2010**, *500*, 26–29.

[25] C. D. Brunetta, W. C. Minsterman, C. H. Lake, J. A. Aitken, *J. Solid State Chem.* **2012**, *187*, 177–185.

[26] F. P. Bundy, J. S. Kasper, *J. Chem. Phys.* **1967**, *46*, 3437–3446.

[27] G. Aminoff, XI. *Z. Kristallogr.* **1923**, *58*, 203–219.

[28] K. A. Rosmus, C. D. Brunetta, M. N. Srnec, B. Karuppannan, J. A. Aitken, *Z. Anorg. Allg. Chem.* **2012**, *638*, 2578–2584.

[29] WINXPOW (version 1.2), STOE & Cie GmbH, Darmstadt (Germany) **2001**.

[30] L. O. Brockway, *Z. Kristallogr.* **1934**, *89*, 434–441.

[31] M. I. Aroyo, J. M. Perez-Mato, D. Orobengoa, E. Tasci, G. de La Flor, A. Kirov, *Bulg. Chem. Commun.* **2011**, *43*, 183–197.

[32] M. I. Aroyo, A. Kirov, C. Capillas, J. M. Perez-Mato, H. Wondratschek, *Acta Crystallogr.* **2006**, *A62*, 115–128.

[33] M. I. Aroyo, J. M. Perez-Mato, C. Capillas, E. Kroumova, S. Ivantchev, G. Madariaga, A. Kirov, H. Wondratschek, *Z. Kristallogr.* **2006**, *221*, 15–27.

[34] O. V. Parasyuk, L. V. Piskach, I. D. Olekseyuk, V. I. Pekhnyo, *J. Alloys Compd.* **2005**, *397*, 95–98.

[35] J. W. Lekse, M. A. Moreau, K. L. McNerny, J. Yeon, P. S. Halasyamani, J. A. Aitken, *Inorg. Chem.* **2009**, *48*, 7516–7518.

[36] J. W. Lekse, B. M. Leverett, C. H. Lake, J. A. Aitken, *J. Solid State Chem.* **2008**, *181*, 3217–3222.

[37] J. Tauc, R. Grigorovici, A. Vancu, *Phys. Stat. Sol. (b)* **1966**, *15*, 627–637.

[38] J. Tauc, *Mater. Res. Bull.* **1968**, *3*, 37–46.

[39] G. E. Davydyuk, G. L. Myronchuk, I. V. Kityk, S. P. Danyl'chuk, V. V. Bozhko, O. V. Parasyuk, *Opt. Mater.* **2011**, *33*, 1302–1306.

[40] H. M. Rietveld, *J. Appl. Crystallogr.* **1969**, *2*, 65–71.

[41] J. Rodríguez-Carvajal, Fᴜʟʟᴘʀᴏꜰ, A Program for Rietveld Refinement and Pattern Matching Analysis, Satellite Meeting on Powder Diffraction of the 15th International Congress of the IUCr, Toulouse (France) **1990**, p. 127.

[42] S. Chen, A. Walsh, Y. Luo, J. Yang, X. G. Gong, S. Wei, *Phys. Rev. B.* **2010**, *82*, 195203-1–195203-8.